Magnetic ordering and spin reorientations in $Nd_{1.8}Sr_{0.2}NiO_{3.72}$

M. Medarde* and J. Rodríguez-Carvajal†
Institut de Ciència de Materials de Barcelona, Consejo Superior de Investigaciones Científicas, Campus Universitari de Bellaterra, 08193-Cerdanyola, Barcelona, Spain and Institut Laue Langevin, Boîte Postale 156, 38042 Grenoble Cedex 9, France

B. Martínez
Institut de Ciència de Materials de Barcelona, Consejo Superior de Investigaciones Científicas, Campus Universitari de Bellaterra, 08193-Cerdanyola, Barcelona, Spain

X. Batlle
Departament de Física Fonamental, Facultat de Física, Universitat de Barcelona, Diagonal 647, 08028 Barcelona, Spain

X. Obradors
Institut de Ciència de Materials de Barcelona, Consejo Superior de Investigaciones Científicas, Campus Universitari de Bellaterra, 08193-Cerdanyola, Barcelona, Spain
(Received 12 October 1993; revised manuscript received 14 December 1993)

The magnetic behavior of the reduced $Nd_{1.8}Sr_{0.2}NiO_{3.72}$ nickelate has been investigated by means of neutron-powder diffraction, magnetic susceptibility, and isothermal magnetization measurements. The most noticeable result is that, in spite of the large concentration of oxygen vacancies, both the Ni and Nd sublattices become antiferromagnetically ordered below $T_{N1} \approx 320$ K and $T_{N2} \approx 13.5$ K, respectively. Moreover, two spin reorientations of the Ni magnetic moments have been observed, one around $T_1 \approx 130$ K and the other simultaneously to the cooperative ordering of the Nd sublattice. The existence of a weak ferromagnetic component below 70 K has also been clearly established from the analysis of the macroscopic magnetic measurements. Finally, a set of effective exchange parameters have been derived, and their values compared with those reported for stoichiometric Nd_2NiO_4.

I. INTRODUCTION

In another paper dealing with the structural aspects of the oxygen-defective $Nd_{1.8}Sr_{0.2}NiO_{3.72}$ nickelate,[1] we reported the existence of several unexpected effects associated with the particular ordering of the oxygen vacancies found in this compound. The first, and perhaps the most noticeable of these effects, was the lowering of the crystallographic symmetry from orthorhombic *Bmab* to monoclinic $B112/n$ (*Cmca* and $C2/c$ in the standard setting).

The second, "microscopic" and slightly more subtle, effect was the appearance of lattice microdistortions produced by the local fluctuations of the oxygen content along the ordering direction of the vacancies. Their existence was signaled by the strong anisotropic broadening of the Bragg reflections, which can be clearly observed in both x-ray- and neutron-powder-diffraction patterns.

This kind of vacancy ordering, which has also been reported for other oxygen-deficient nickelates of the $La_{2-x}Sr_xNiO_{4+\delta}$ ($\delta < 0$) series,[2-4] is expected to also have important consequences in both the electronic and magnetic properties of these compounds. Unfortunately, only very few published works dealing with the physical properties of these reduced systems are nowadays available.

As a continuation of the previous structural characterization,[1] we present here an exhaustive magnetic study of $Nd_{1.8}Sr_{0.2}NiO_{3.72}$. Neutron-diffraction, ac and dc susceptibility, and isothermal magnetization measurements have been used to obtain an overall picture of its magnetic behavior, including the characterization of several spin reorientations observed in this compound, the determination of the subsequent magnetic structures, and the obtainment of a set of effective magnetic interactions. The influence of the crystallographic symmetry and the ordering of the oxygen vacancies are also briefly discussed and compared with the results obtained for Nd_2NiO_4.

II. EXPERIMENTAL TECHNIQUES

About 5 g of a dark-brown polycrystalline sample of composition $La_{1.8}Sr_{0.2}NiO_{3.72}$ were synthesized in accordance with the procedure described in Ref. 1. The x-ray- and neutron-diffraction characterization reported in this work showed that the material has a K_2NiF_4-type structure of monoclinic $B112/n$ symmetry. The oxygen vacancies ($\delta = 0.28$) are localized in the basal planes of the NiO_6 octahedra (see Fig. 6 of Ref. 1) and partially ordered along the [110] crystallographic direction. In fact, a slightly different composition was published in a short preliminary study,[5] but more careful investigations[1] indicated that the correct oxygen stoichiometry is $\delta = 0.28$.

Several neutron-diffraction experiments were per-

formed at the high-flux reactor of the Institut Laue-Langevin as described in Ref. 1. dc magnetic susceptibility and isothermal magnetization measurements were carried out using a Quantum Design SHE superconducting quantum interference device (SQUID) magnetometer in a temperature range from 4.5 to 350 K with magnetic fields up to 50 kOe. The isothermal magnetization curves at different temperatures were measured on decreasing the magnetic field from 55 kOe. ac magnetic susceptibility was carried out in a LakeShore ac susceptometer between 4.5 K and room temperature (RT). A small amount of metallic nickel ($\approx 0.3\%$ in weight) was detected from isothermal magnetization curves. This impurity was probably formed during the hydrogen-reduction step and was undetectable in both x-ray- and neutron-diffraction patterns.

III. NEUTRON DIFFRACTION

A. Results

Figure 1(a) shows the low-angle part of the neutron-powder-diffraction patterns of $Nd_{1.8}Sr_{0.2}NiO_{3.27}$ recorded at 200 K. A comparison with previous high-temperature data indicates the existence of several additional reflections, all of them indexable on the crystallographic unit cell. The Miller indices fulfill the parity rule $p(h)\neq p(k)=p(l)$, and they are in consequence forbidden by the general extinction conditions of the $B112/n$ space group hkl, $h+l=2n$; $hk0$, $h,k=2n$; $0kl$, $l=2n$; $h0l$, $h+l=2n$; $00l$, $l=2n$; $h00$, $h=2n$; $0k0$, $k=2n$. A similar situation is found in Fig. 1(b), where the neutron-powder-diffraction pattern recorded at 16.5 K is displayed. The only extra feature is the appearance of a new, very small reflection at $2\theta\approx 27°$, also forbidden by the $B112/n$ crystallographic symmetry.

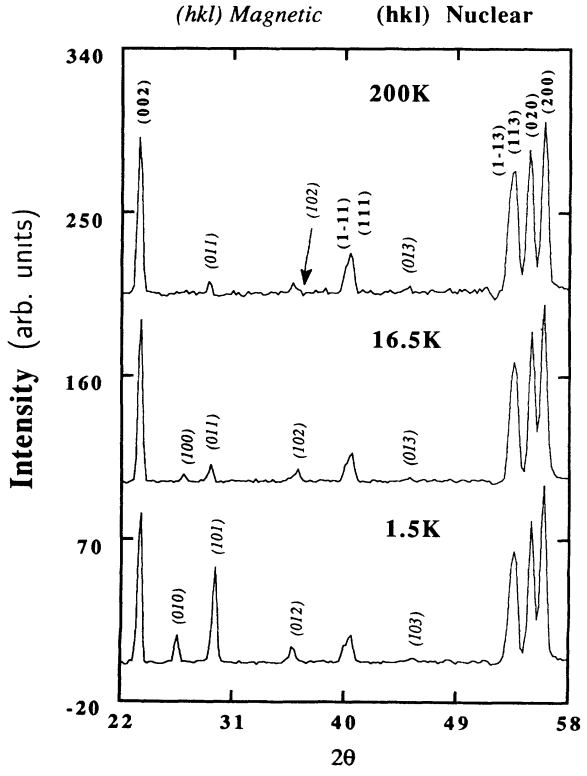

FIG. 1. Low-angle part of neutron-powder-diffraction patterns for $Nd_{1.8}Sr_{0.2}NiO_{3.72}$ at 200, 16.5, and 1.5 K.

Figure 1(c) shows the neutron-diffraction pattern at 1.5 K. Looking carefully at the position of the peaks, it is straightforward to see that the (100), (011), (102), and (013) reflections, which are clearly observable at 16.5 K, have been substituted by the (010), (101), (012), and (103) reflections. All of them are characterized by equal h and l parities $p(h)=p(l)\neq p(k)$ and, with the exception of (010), are allowed by the general extinction condition of the crystallographic space group. Note, however, that although this last reflection is forbidden by the n plane, it is allowed by the B centering.

The substitution of the $p(h)\neq p(k)=p(l)$ by the $p(h)=p(l)\neq p(k)$ set is more clearly shown in Fig. 2, where the thermal evolution of the center of gravity of the (100)-(010), (011)-(101), and (102)-(012) pairs is

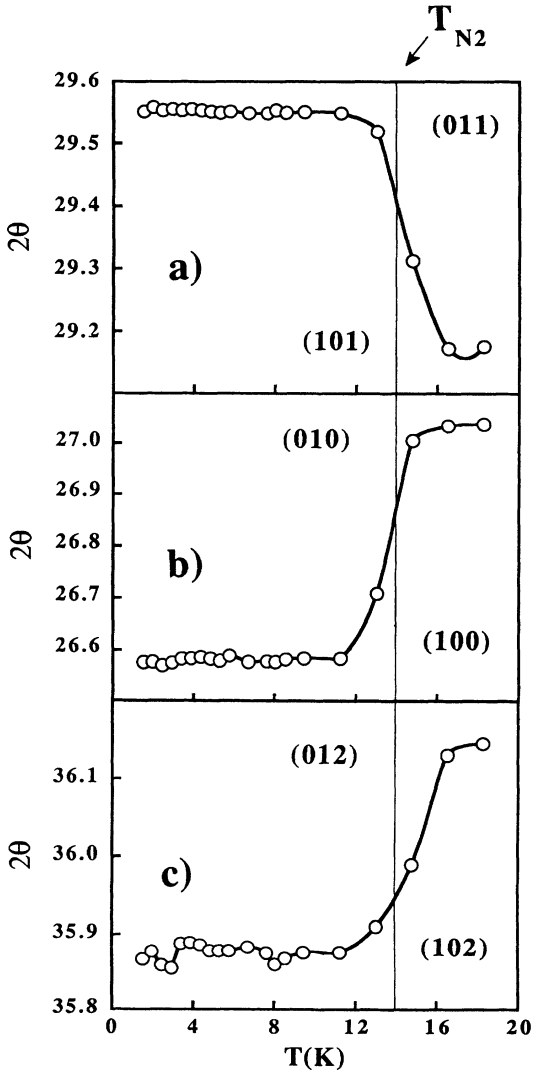

FIG. 2. Thermal evolution of the center of gravity of the (a) (011)-(101), (b) (100)-(010), and (c) (102)-(012) pairs of magnetic reflections. The solid lines are guides for the eye.

displayed. Taking as transition temperature that at which the 2θ variation is maximal, the observed changes would take place at $T_{N2} \approx 13.5$ K.

Figures 3(a), 3(b), and 3(c) show the evolution of the integrated intensity of the (100)-(010), (011)-(101), and (102)-(012) reflections between RT and 1.5 K. Although their nature cannot be unambiguously established without carrying out a polarization analysis, their characteristic temperature dependence suggests that all of them are magnetic in origin.

Let us now consider the high-temperature [open circles, $p(h) \neq p(k) = p(l)$ parities] and low-temperature [solid circles, $p(h) = p(l) \neq p(k)$ parities] sets separately. Concerning the first set, their relatively weak intensities, as well as the high (extrapolated) temperature at which they vanish ($T_{N1} \approx 320$ K) suggest that, as in $Nd_2NiO_{4.00}$, a cooperative antiferromagnetic ordering of the Ni sublattice takes place at this temperature. Note, however, that the (100) magnetic reflection appears only between 100 and 150 K, indicating the possible existence of an additional reorientation of the Ni magnetic moments between these two temperatures.

The low-temperature set of reflections is probably related to the cooperative ordering of the Nd^{3+} sublattice. This origin is suggested by their high intensity, as well as by the decrease of the paramagnetic scattering contribution on the low-temperature neutron-diffraction patterns.

In $Nd_2NiO_{4.00}$, the cooperative ordering of the Nd^{3+} magnetic moments was also observed in this temperature range ($T_{N2} \approx 12$ K).[6] However, no evidence of a similar reorientation could be detected simultaneously to the Nd^{3+} ordering. In fact, the (100)-(010), (011)-(101), or (102)-(012) reflections in this compound are superimposed below 130 K because of its low-temperature $P4_2/ncm$

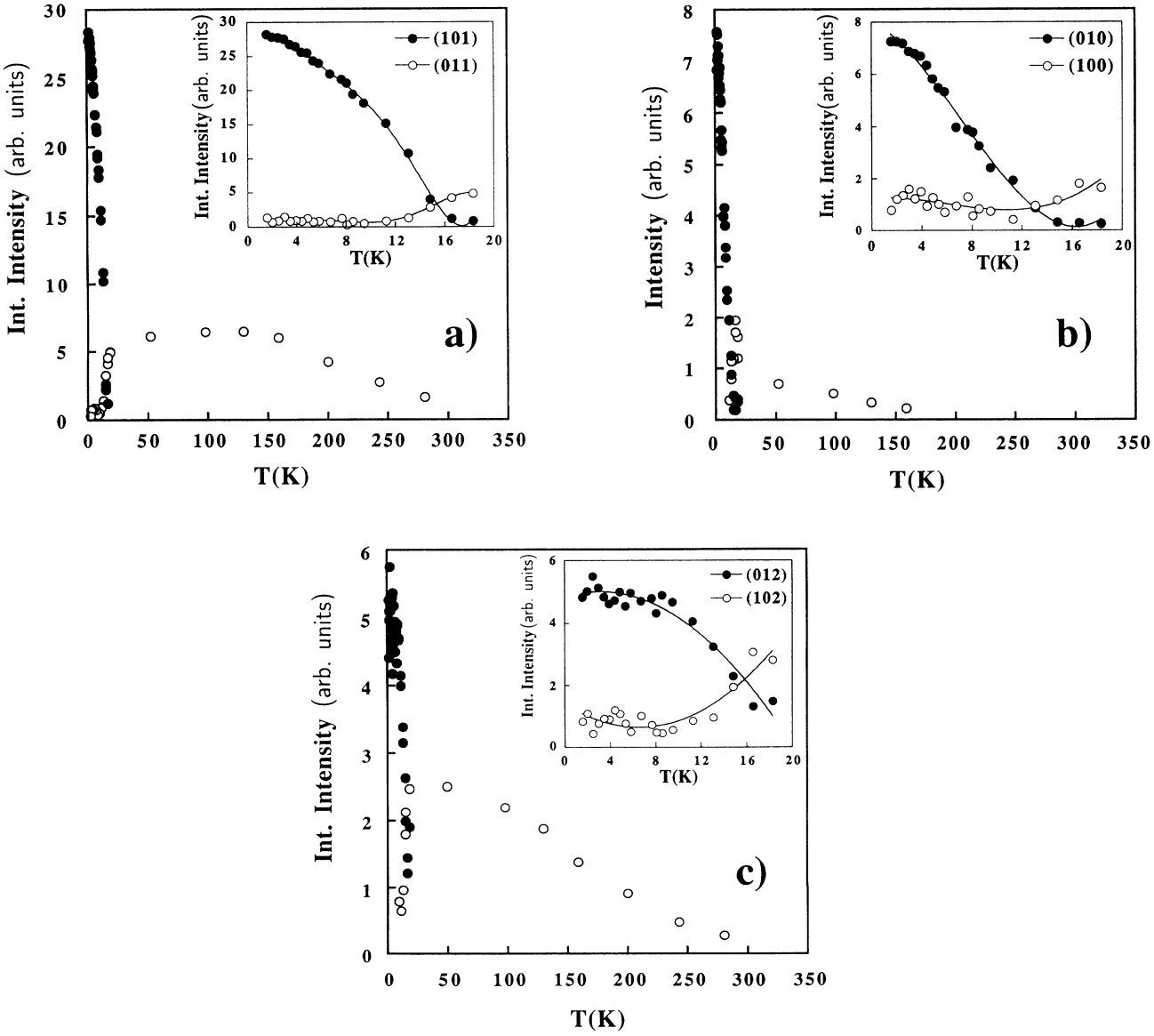

FIG. 3. Thermal evolution of the integrated intensities of some magnetic reflections: (a) (011)-(101), (b) (100)-(010), and (c) (102)-(012). The solid lines are guides for the eye.

symmetry. Then, if such a spin reorientation exists in the stoichiometric compound, single-crystal experiments under uniaxial stress would be necessary to make it evident.

Another important difference between $Nd_2NiO_{4.00}$ and $Nd_{1.8}Sr_{0.2}NiO_{3.72}$ is that, in the undoped compound, the polarization of the Nd sublattice in the exchange field produced by the Ni^{2+} magnetic moments in the Nd sites is clearly observable below 70 K. In $Nd_{1.8}Sr_{0.2}NiO_{3.72}$, no appreciable increase of the magnetic intensities can be observed below this temperature (see Fig. 3). This behavior indicates that the Ni-Nd exchange field is probably affected by the disorder introduced in the Ni sublattice by the oxygen vacancies. Note that, even if the magnetic reflections can be reproduced by supposing the existence of an average Ni magnetic moment (see Sec. III C), its local value fluctuates from one site to another depending on the spatial distribution of oxygen vacancies.

Finally, it is worth mentioning that no appreciable changes in the integrated intensity of the purely nuclear reflections have been observed in the studied temperature range, apart from those associated with the thermal evolution of the crystallographic structure. This finding is also in contrast with the behavior found in $Nd_2NiO_{4.00}$, where the sudden appearance of additional intensity in the (111) nuclear reflection below 20 K has been interpreted as an enhancement of the ferromagnetic component along the c axis existing at higher temperatures.[7] Because of its smallness, this ferromagnetic component was invisible for neutrons between 130 and 20 K, but its existence was unambiguously determined by means of isothermal magnetic measurements. In the case of the $Nd_{1.8}Sr_{0.2}NiO_{3.72}$ compound, the same macroscopic measurements are also conclusive about the existence of a weak ferromagnetic component below 70 K (see Sec. IV A). Its magnitude ($0.27\mu_B$) is much smaller than the value found in the stoichiometric compound ($1.02\mu_B$),[7] and for that reason it is undetectable in our neutron-powder-diffraction data.

B. Group-theory analysis

In order to get further insight about the nature of the spin reorientations associated with the observed changes in the magnetic intensities, we have carried out a group-theoretical analysis of the possible magnetic structures compatible with the $B112/n(C2/c)$ symmetry. As all the magnetic reflections can be indexed with the crystallographic unit cell, the reduced propagation vector of the magnetic structure can be taken as $\mathbf{k}=[000]$. However, the extinction conditions discussed in Sec. III A show unambiguously that, between T_{N1} and T_{N2}, the *magnetic lattice is not centered.* Thus the propagation vector in this temperature range is $\mathbf{k}=[100]$ [see Fig. 4(a)]. Below T_{N2}, the *magnetic lattice becomes B centered* ($h+l=2n$ for all hkl) and, in consequence, $\mathbf{k}=[000]$. This situation is schematically shown in Fig. 4(b).

The relevant irreducible representations which take into account both propagation vectors are those of the point group of $B112/n(2/m)$, properly modified by the addition of the characters corresponding to the B centering. The possible magnetic structures were deduced using the macroscopic theory of Bertaut.[20] The Ni atoms in the unit cell were labeled as $Ni_1(0,0,0)$, $Ni_2(\frac{1}{2},0,\frac{1}{2})$, $Ni_3(0,\frac{1}{2},\frac{1}{2})$, and $Ni_4(\frac{1}{2},\frac{1}{2},0)$ [Wyckoff position (4a)]. Note that this labeling is the same as that in previous papers.[7] The basis vectors of the one-dimensional (1D) representations of the space group $B112/n$ can be constructed from the linear combinations

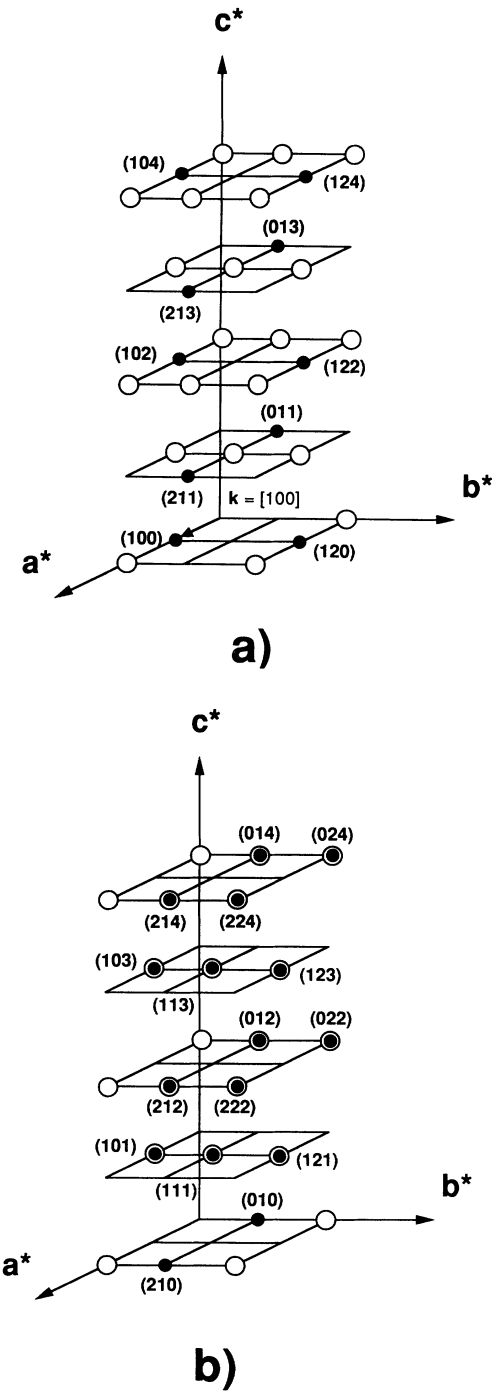

FIG. 4. Portion of the reciprocal space showing the reflections allowed by the $B112/n$ space group (open circles) and the observed magnetic reflections (solid circles). (a) $T_{N2} \leq T \leq T_{N1}$, and (b) $T < T_{N2}$. For clarity, arbitrary dimensions have been used for the modulus of the $\mathbf{a}^*$, $\mathbf{b}^*$, and $\mathbf{c}^*$ reciprocal cell parameters.

TABLE I. Conditions ruling the existence of magnetic reflections for the *f*, *a*, *c*, and *g* modes (Ni positions).

f	$p(h)=p(k)=p(l)$
a	$p(h)=p(k)\neq p(l)$
g	$p(h)\neq p(k)=p(l)$
c	$p(h)=(p(l)\neq p(k)$

$$\mathbf{f}=\mathbf{s}_1+\mathbf{s}_2+\mathbf{s}_3+\mathbf{s}_4\ ,\quad \mathbf{a}=\mathbf{s}_1-\mathbf{s}_2-\mathbf{s}_3+\mathbf{s}_4\ ,$$
$$\mathbf{g}=\mathbf{s}_1-\mathbf{s}_2+\mathbf{s}_3-\mathbf{s}_4\ ,\quad \mathbf{c}=\mathbf{s}_1+\mathbf{s}_2-\mathbf{s}_3-\mathbf{s}_4\ . \tag{1}$$

The generators (modulo integer translations) of the $B112/n$ space group are $(\bar{1},B,2_z)$, where the notation stands for the inversion center at the origin, the $(\frac{1}{2},0,\frac{1}{2})$ centering, and the binary $(\frac{1}{4},\frac{1}{4},z)$ axis. The one-dimensional representations of $B112/n$ can be labeled by the characters corresponding to the generators. However, as the point symmetry of the Ni sites is $\bar{1}$, the spin configurations are invariant under the inversion center and only the even (gerade) representations are relevant, that is, $\Gamma_{1g}(++)$, $\Gamma_{2g}(+-)$, $\Gamma_{3g}(-+)$, and $\Gamma_{4g}(--)$. The magnetic modes, Shubnikov groups, and the conditions ruling the existence of magnetic reflections for each magnetic mode are summarized in Tables I and II.

The Nd atoms were divided in two sets: (a) $Nd_1(0,0,z)$, $Nd_2(\frac{1}{2},0,\frac{1}{2}-z)$, $Nd_3(0,\frac{1}{2},\frac{1}{2}-z)$, $Nd_4(\frac{1}{2},\frac{1}{2},z)$ and (b) $Nd_{1'}(0,0,-z)$, $Nd_{2'}(\frac{1}{2},0,\frac{1}{2}+z)$, $Nd_{3'}(0,\frac{1}{2},\frac{1}{2}+z)$, $Nd_{4'}(\frac{1}{2},\frac{1}{2},-z)$, where the *y* coordinates have been omitted for clarity. The prime denotes atoms related by an inversion center. Note that this classification is again the same as that in Ref. 7. For every set we can use the same labeling of magnetic modes as that in the Ni case. The coupling between the two sets results in the linear combinations

$$\mathbf{F}=\mathbf{f}+\mathbf{f}'\ ,\quad \mathbf{G}=\mathbf{g}+\mathbf{g}'\ ,\quad \mathbf{C}=\mathbf{c}+\mathbf{c}'\ ,\quad \mathbf{A}=\mathbf{a}+\mathbf{a}'\ ,$$
$$\mathbf{P}=\mathbf{f}-\mathbf{f}'\ ,\quad \mathbf{Q}=\mathbf{g}-\mathbf{g}'\ ,\quad \mathbf{R}=\mathbf{c}-\mathbf{c}'\ ,\quad \mathbf{L}=\mathbf{a}-\mathbf{a}'\ . \tag{2}$$

The magnetic modes and Shubnikov groups for each representation are summarized in Table II. Note that in this case and because the Nd atoms are located in general positions, no conditions ruling the existence of magnetic reflections can be derived.

TABLE II. Magnetic modes for Ni and Nd sites in the $B112/n$ space group. The *j* representation is labeled by the symbol Γ_j. The + and − symbols in parentheses correspond to the characters +1 or −1 of the space-group generators. The character of the inversion center is omitted, being substituted by the subscript *g*/*u* (gerade/ungerade) for the +1 (even) or −1 (odd) representation. Nd atoms are placed in general positions; then, no general conditions limiting the existence of magnetic reflections can be obtained. If a magnetic structure can be described, for instance, by the (f_x,f_y,c_z) basis function belonging to the $\Gamma_{2g}(+-)$ representation, the four Ni atoms of the unit cell will show the following magnetic moments: Ni_1, (μ_x,μ_y,μ_z); Ni_2, (μ_x,μ_y,μ_z); Ni_3, $(\mu_x,\mu_y,-\mu_z)$; and Ni_4, $(\mu_x,\mu_y,-\mu_z)$.

(a) Ni in $B112/n$ $\{B,2_z\}$		*x*	*y*	*z*
$\Gamma_{1g}(++)$	$B112/n$	c_x	c_y	f_z
$\Gamma_{2g}(+-)$	$B112'/n$	f_x	f_y	c_z
$\Gamma_{3g}(-+)$	B_p112/n'	g_x	g_y	a_z
$\Gamma_{4g}(--)$	B_p112'/n'	a_x	a_y	g_z
(b) Nd in $B112/n$ $\{B,2_z\}$		*x*	*y*	*z*
$\Gamma_{1g}(++)$	$B112/n$	C_x	C_y	F_z
$\Gamma_{2g}(+-)$	$B112'/n'$	F_x	F_y	C_z
$\Gamma_{3g}(-+)$	B_p112/n	G_x	G_y	A_z
$\Gamma_{4g}(--)$	B_p112'/n'	A_x	A_y	G_z
$\Gamma_{1u}(++)$	$B112/n'$	Q_x	Q_y	L_z
$\Gamma_{2u}(+-)$	$B112'/n$	L_x	L_y	Q_z
$\Gamma_{3u}(-+)$	B_p112/n'	R_x	R_y	P_z
$\Gamma_{4u}(--)$	B_p112'/n	P_x	P_y	R_z

C. Determination of the magnetic structures

1. Ni sublattice between T_{N1} and T_{N2}

As was pointed out in former sections, the Miller indices of all the reflections observed between T_{N1} and T_{N2} exhibit $p(h)\neq p(k)=p(l)$ parities, which are characteristic of a *g* mode. Then only the $\Gamma_{3g}(-+)$ and $\Gamma_{4g}(--)$ representations, which contain, respectively, the g_xg_y and g_z modes, are possible. To decide between these two spin arrangements, we have calculated their magnetic powder-diffraction patterns using a reasonable value of $1.6\mu_B$ for the total magnetic moment of Ni. These calculations indicate that, even if the $(g_x,g_y,0)$ and $(0,0,g_z)$ configurations give rise to the *same* magnetic reflections, their intensities are substantially different. Then a comparison with the experimental data unambiguously supports the $(g_x,g_y,0)$ mode.

If an a_z component, which is also allowed by the $\Gamma_{3g}(-+)$ representation, were also active, several $p(h)=p(k)\neq p(l)$ reflections as, for example, (110) would be also present. However, none of them have been observed in the neutron-powder-diffraction patterns, at least within our experimental resolution. This fact is confirmed by the Rietveld refinement of the magnetic structure [see Fig. 5(a)], that, within the error, was unable to detect the existence of such a component.

The refined value for the magnetic moments in the Ni sites (μ^{Ni}) is displayed in Fig. 6(a). From RT to ≈ 130 K, they are oriented along the *a* axis and the magnetic structure is the same as reported for Nd_2NiO_4 in this range of temperatures [see Fig. 7(a)]. Thus the lower crystallographic symmetry and the partially ordered oxygen vacancies of $Nd_{1.8}Sr_{0.2}NiO_{3.72}$ do not seem to affect very much the magnetic interactions which are responsible for the magnetic ordering in the undoped stoichiometric compound. Additional facts supporting this conclusion are presented in Sec. IV.

At $T\approx T_1\approx 130$ K, the (100) reflection, which has an appreciable intensity only when a μ_y^{Ni} magnetic moment component along the *b* axis exists, starts to develop. At the same time, a reduction of the μ_x^{Ni} component is observed below this temperature. At $T_2\approx 16.5$ K, both μ_x^{Ni} and μ_y^{Ni} have the same magnitude and, as a result, the direction of the magnetic moments changes from [100] to [110] [see Figs. 7(a) and 7(b)].

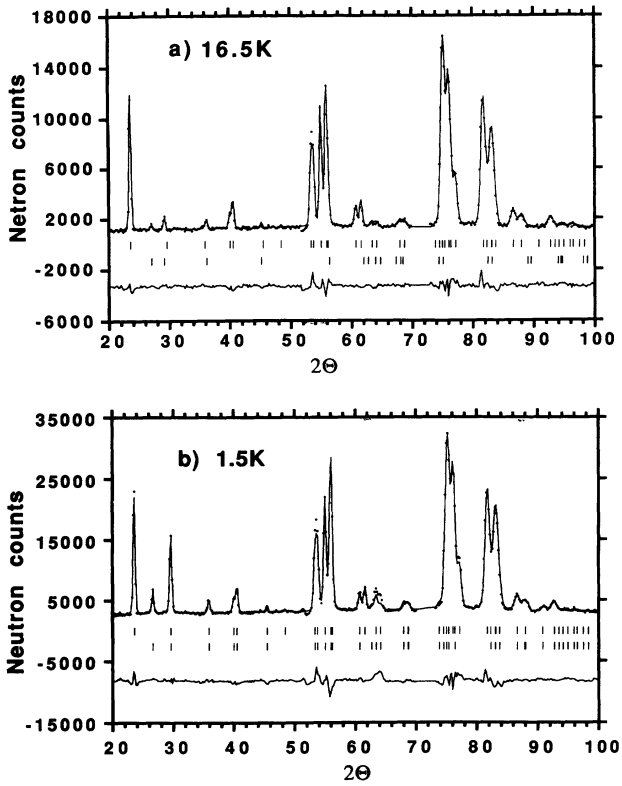

FIG. 5. Observed and calculated neutron-powder-diffraction patterns at 16.5 and 1.5 K. The first row of ticks corresponds to the nuclear reflections and the second row to the magnetic reflections allowed by (a) the $(g_x,g_y,0)$ mode of Ni and (b) the $(c_x,c_y,0)$ of Ni + the $(C_x,C_y,0)$ mode of Nd.

From a more general point of view, the magnetic structure of the Ni^{2+} sublattice between $T_{N1}\approx 320$ K and $T_{N2}\approx 13.5$ K can be described as a coherent superposition of both La_2NiO_4 $(g_x,0,0)$ and La_2CuO_4 $(0,g_y,a_z)$ modes. From T_{N1} to T_1, the amplitude of the $(0,g_y,a_z)$ mode is zero. Below T_1 and probably as a consequence of the smooth decrease of the monoclinic strain $s=2(b-a\sin\gamma)/(b+a\sin\gamma)$ which takes place between T_1 and T_2,[1] both modes coexist. As the temperature decreases, the $(0,g_y,a_z)$ amplitude increases and that of $(g_x,0,0)$ decreases to become nearly equal to $T_2\approx 16.5$ K. In La_2CoO_4, a very similar magnetic reorientation, also driven by a structural phase transition, has been described.[8] The main difference is that in the latter compound the low-temperature magnetic structure is purely of La_2CuO_4 type. The coexistence found in our sample is likely attributable to the sluggish nature of the structural changes observed between T_1 and T_2.

The next point for an understanding of the spin reorientation would be trying to relate the observed changes in the spin direction with the evolution of the crystallographic parameters across the transition. Unfortunately and because of the smallness of these changes, it was not possible to obtain any conclusive result in the previously published structural neutron-diffraction study; within the resolution of the D1B diffractometer, the tilt axis of the NiO_6 octahedra, which is [100] between RT and T_1, remains unchanged below this temperature.

On the other hand, it is interesting to observe that, in the high-temperature orthorhombic phase of Nd_2NiO_4 and $Nd_{1.95}Sr_{0.05}NiO_4$,[4,7] where the NiO_6 octahedra rotate about the [100] direction, the orientation of the magnetic moments is coincident with the tilt axis. As for $Nd_{1.8}Sr_{0.2}NiO_{3.72}$, these two compounds undergo a structural phase transition at $T_{C1}\approx 130$ and 118 K, respectively, which is characterized by a sudden change of the tilt axis from the [100] to the [110] direction. The low-temperature phase is tetragonal $P4_2/ncm$ in the case of Nd_2NiO_4, and in consequence it is not possible to separate the μ_x and μ_y components. However, the orthorhombic $Pccn$ low-temperature symmetry of $Nd_{1.95}Sr_{0.05}NiO_4$ allows the determination of the absolute

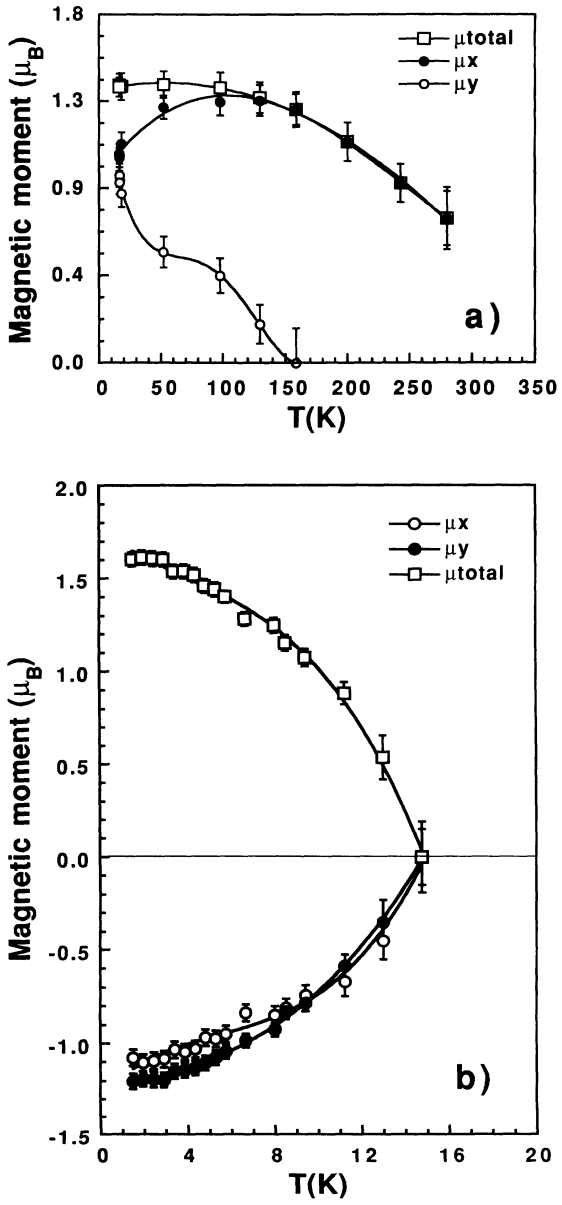

FIG. 6. (a) Temperature dependence of the Ni_1 magnetic moment. (b) The same for the Nd_1 magnetic moment refined using the model (1) for the magnetic structure [see Fig. 7(c)]. The solid lines are guides for the eye.

direction of the magnetic moments, which is again coincident with that of the tilt axis. Thus we can speculate that the spin reorientation observed in our sample is probably related to a sluggish change of the octahedra's tilt axis between these two directions, probably too small to be observed in our medium-resolution data. Further high-resolution experiments will be necessary in order to confirm this hypothesis.

Concerning now the refined values of the Ni magnetic moment, Fig. 6(a) shows that, at 16.5 K, the total magnetic moment in the Ni sites is $1.43(1)\mu_B$. This value is smaller than that refined in stoichiometric $Nd_2NiO_{4.00}$ ($1.57\mu_B$), which was also reduced with respect to the spin-only free-ion value of Ni^{2+} (high spin, $2\mu_B$) because of the quasibidimensionality of the K_2NiF_4-type structure and covalency effects. In our case, the small enhancement of the $c/\langle a,b \rangle$ ratio observed in $Nd_{1.8}Sr_{0.2}NiO_{3.72}$ (2.27) with respect to Nd_2NiO_4 (2.20) (3%) cannot account for the observed reduction of the Ni magnetic moment (−9%). Thus the most probable origin is the formal mixed valence Ni^+/Ni^{2+} of $Nd_{1.8}Sr_{0.2}NiO_{3.72}$, which, in a completely ionic approximation, would suppose the existence of 64% of Ni^+ and 36% of Ni^{2+}.

The breaking of the superexchange Ni-O-Ni paths should also be considered. It is interesting to note that simple topological considerations can give an upper limit for the number of oxygen vacancies which allow the existence of at least an infinitely connected path for superexchange interactions. For a quadratic lattice (topologically equivalent to our monoclinically distorted NiO_2 planes), this limit is 43%,[9] that is, far bigger than the actual number of vacancies found in our sample, where only 14% of the basal oxygen positions are unoccupied.

2. *Ni and Nd sublattices between 1.5 K and T_{N2}*

As no condition limiting the existence of magnetic reflections can be derived for the Nd sublattice, the determination of the low-temperature magnetic structure requires the test of all the possible combinations between the Ni and Nd magnetic modes. Simulations of the neutron-diffraction patterns by coupling modes belonging to the same representation show that only four of them allow the existence of the observed $p(h)=p(l)\neq p(k)$ Bragg reflections. The best Rietveld refinement was obtained for the (c_x,c_y,f_z) (Ni) and (C_x,C_y,F_z) (Nd) modes, both belonging to the $\Gamma_{1g}(++)$ representation of $B112/n$.

As can be observed in Fig. 5(b), some discrepancies between the experimental and calculated patterns exist. Thus additional tries were made by combining modes belonging to different irreducible representations. As no better agreement could be obtained, an exploration of all possible spin configurations compatible with the observed magnetic intensities was made by using a "simulating annealing" procedure.[10] Surprisingly, we found that the modes (c_x,c_y,f_z) (Ni) and (C_x,C_y,F_z) (Nd) behave as a strong attractor, the other magnetic arrangements providing always worse reliability factors. Thus we believe that the magnetic structure of $Nd_{1.8}Sr_{0.2}NiO_{3.72}$ below T_{N2} can be basically described with this model, the deviations being probably due to the local disorder introduced by the Sr substitution and oxygen vacancies.

As the modes acting along the x and y directions are of the same type and that acting along the z direction is ferromagnetic, the arrangement of the magnetic moments of each sublattice is collinear, irrespective of their absolute orientations. Concerning the coupling between both sub-

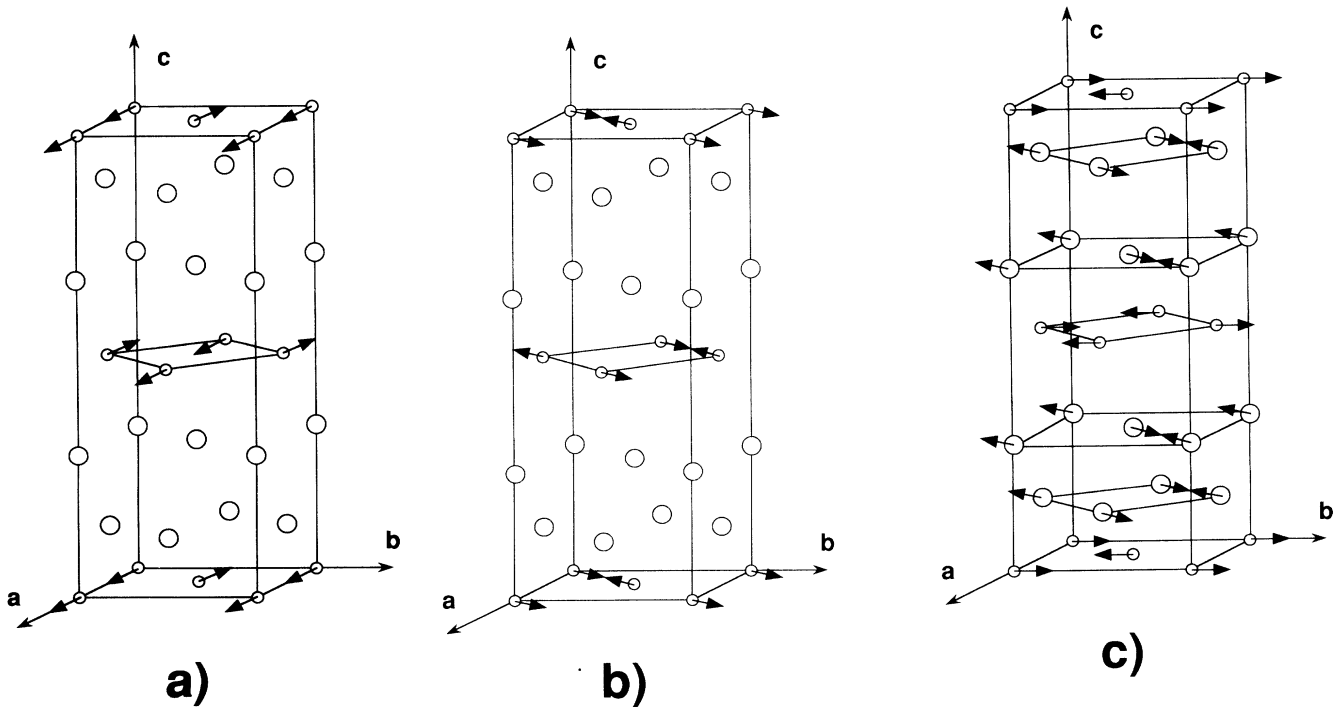

FIG. 7. Proposed magnetic structure for $Nd_{1.8}Sr_{0.2}NiO_{3.72}$. (a) $T_{N1} > T > T_{C1}$, $(g_x,0,0)$ mode; (b) $T_{C1} > T > T_{N2}$, $(g_x,g_y,0)$ mode; (c) $T < T_{N2}$, $(c_x,c_y,0)$ and $(C_x,C_y,0_z)$ modes for the Ni and Nd sublattices, respectively.

lattices, the Rietveld refinements indicate that two possibilities give approximately the same reliability factors. In the first of them, schematically displayed in Fig. 7(c), the Ni moments point along the b axis forming an angle of 135° with the ordering direction of the Nd sublattice. In the second possibility, the Ni moments are oriented along the [110] direction, the angle between the Ni and Nd sublattices being approximately the same as in the former case.

The most interesting feature of this low-temperature magnetic structure is that, in contrast with the behavior found in the high-temperature region ($T_{N2} \leq T \leq T_{N1}$), the arrangement of the Ni and Nd magnetic moments is now substantially different than that reported for Nd_2NiO_4 below T_{N2} [(g_x,c_y,f_z) (Ni) and (G_x,C_y,F_z) (Nd)]. Thus the structural and electronic changes produced by the Sr doping and the oxygen vacancies seem to affect predominantly the Nd-Nd and/or Ni-Nd interactions, the Ni-Ni magnetic coupling being in principle less sensitive to this kind of defects.

Figure 6(b) shows the temperature dependence of the μ_x^{Nd} and μ_y^{Nd} components of the magnetic moment for the Nd atom situated in (0, −0.008, 0.3626), as well as that of its modulus. In $Nd_2NiO_{4.00}$, no information about the actual direction of the in-plane magnetic moment of the rare earth can be derived because of its average low temperature tetragonal symmetry. In our case and because of the monoclinic symmetry of $Nd_{2-x}Sr_xNiO_{3.72}$, it is possible to separate both μ_x^{Nd} and μ_y^{Nd} components. Concerning the existence of a ferromagnetic component along the c direction, which is also allowed by the modes $(c_x,c_y,f_z)+(C_x,C_y,F_z)$, no clear conclusion could be derived from our present data. However, its existence is clearly demonstrated from the analysis of the isothermal magnetization measurements (see Sec. IV).

At 1.5 K, the refined magnetic moment in the Nd sites is $1.60\mu_B$. Although a reduction from $3.27\mu_B$ to $2.95\mu_B$ would be expected from the substitution of 10% of the Nd^{3+} ions by diamagnetic Sr^{2+}, the observed decrease is too important to be due only to this effect. An additional mechanism which can contribute to this reduction is the change in the crystalline electric field on the rare-earth sites as a consequence of the different charge and size of the Nd^{3+} and Sr^{2+} cations. Even if a quantitative estimation of this effect is out of the scope of this work, important changes of the crystal-field splitting of the J multiplet of the Nd^{3+} would be expected, which can affect the saturation value of the Nd^{3+} magnetic moment.

IV. MACROSCOPIC MAGNETIC MEASUREMENTS: RESULTS

The results of the dc and ac susceptibility measurements as well as the study of the isothermal magnetization process confirm the overall picture of the magnetic transitions observed by neutron-powder diffraction.

The dc susceptibility χ_{dc} as a function of temperature, measured at 10 kOe, is shown in Fig. 8. The different magnetic transitions described in the previous sections are indicated in the curve, although the expected anomalies associated with the 3D ordering and the reorientations of the Ni sublattice at T_{N1}, T_1, and T_2, are completely masked by the large contribution of the paramagnetic Nd^{3+} ions. At approximately $T_3 \approx 12$ K, we observe a maximum on the $\chi_{dc}(T)$ curve which may be attributed to the 3D long-range ordering of the Nd^{3+} sublattice. Note that this temperature is the same as in the undoped $Nd_2NiO_{4.00}$ sample,[6] but higher than that observed at the T' cuprates [T_N (Nd^{3+}) = 1.5 K in Nd_2CuO_4 (Ref. 11)]. Note also that in the neutron-powder-diffraction experiments, $T_3 \approx 12$ K corresponds to the point at which the $(g_x,g_y,0) \rightarrow (c_x,c_y,\phi)$ magnetic transition is completely accomplished and not the temperature at which a maximum transformation rate is achieved ($T_{N2} \approx 13.5$ K).

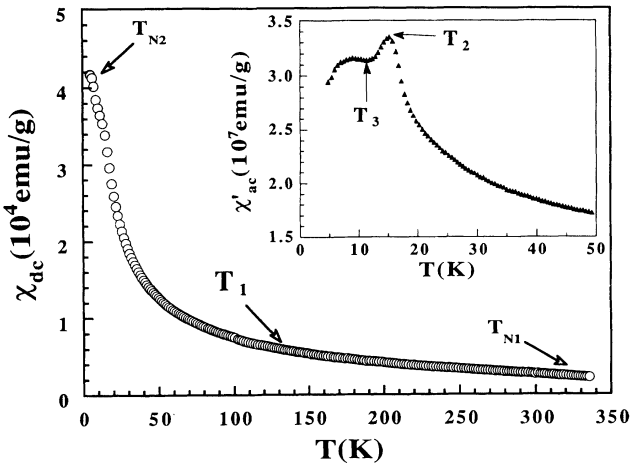

FIG. 8. dc susceptibility χ_{dc} as a function of the temperature obtained under an external applied field $H_a = 10$ kOe. The transition temperatures of the Ni (T_{N1}) and Nd (T_{N2}) magnetic sublattices are indicated. Inset: real part of the ac susceptibility (χ'_{ac}) in the low-temperature range showing the in-plane reorientation of the Ni^{2+} moments and the appearance of the long-range antiferromagnetic ordering of the Nd^{3+} moments.

The maximum at T_3 is also detected in the low-field ac susceptibility measurements as a local minimum (see inset of Fig. 8), together with an additional maximum at 16.5 K. This temperature corresponds to the end of the $(g_x,0,0) \rightarrow (g_x,g_y,0)$ transformation T_2, which is the temperature at which the spin reorientation of the Ni magnetic moments is finished. Below T_{N2} there is an enhancement of the weak ferromagnetic components in both Nd^{3+} and Ni^{2+} sublattices (see next sections). Also, an anomalous T dependence of $\chi'_{ac}(T)$ is observed, which may reflect a complex behavior of the domain walls that are tested at such low magnetic fields. It should be emphasized that no traces of a peak are detected in the imaginary part (χ''_{ac}) of the susceptibility at 16.5 K, while a small peak is indeed observed around 12 K (not shown in the figure).

In Fig. 9 are shown several isothermal magnetization curves measured between 4.5 K and RT. The hysteresis curve at 4.5 K is also shown in Fig. 10, where it is evident that the coercive field is very small (around 200 Oe). This is in strong contrast with $Nd_2NiO_{4.00}$, where we observed a coercive field higher than 10 kOe at 4.5 K,[6] but similar

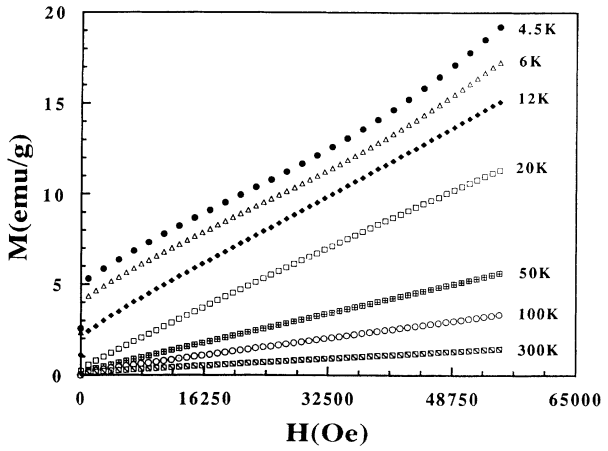

FIG. 9. Isothermal magnetization curves for several temperatures measured on decreasing the magnetic field from 55 kOe.

in magnitude to that observed in $La_2NiO_{4.00}$ (0.7 kOe at 4.5 K).[12] The origin of such a large difference will be addressed later in the discussion. As can be clearly seen in Fig. 9, the high-temperature-range magnetization curves have a linear field dependence showing no remanence at all, as expected for the $(g_x,g_y,0)$ antiferromagnetic mode. However, below approximately 70 K a *small spontaneous magnetization starts to appear* and the magnetic properties of the system change, showing the typical features of a weak ferromagnetic behavior with a strong increase of the remanent magnetization and the appearance of a coercive field (around 200 Oe at 4.5 K) below $T \approx 20$ K.

These features suggest the development of a weak ferromagnetic spin component with a domain structure (see the hysteresis between the virgin magnetization curve and the decreasing branch of the hysteresis loop at 4.5 K displayed in Fig. 10). We note that no anomalous drops are observed in the magnetization curve when the field is inverted, in contrast with the behavior observed in the stoichiometric $Nd_2NiO_{4.00}$. This fact suggests that the domain walls associated with the ferromagnetic spin component are broad (small anisotropy), which is in

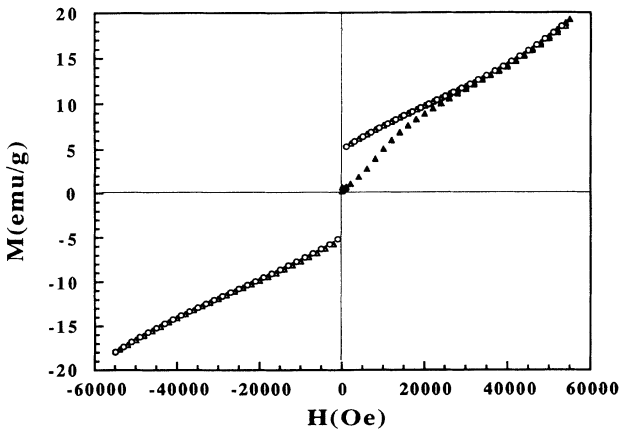

FIG. 10. Hysteresis curve obtained at $T=4.5$ K (△,○); the virgin magnetization curve is also included (▲).

agreement with the experimental values observed for the coercive field.

As was pointed out in previous sections, no ferromagnetic component could be refined in the neutron-powder-diffraction patterns. Moreover, its existence is formally forbidden by the $(g_x,g_y,0)$ mode, which is active in the $T_{N2} < T < T_{N1}$ temperature range. Three possible explanations for this anomalous behavior can be given. The first is that the coexistence of the low-temperature (c_x,c_y,f_z) mode (which allows the existence of a ferromagnetic component along the c axis) and the high-temperature mode $(g_x,g_y,0)$ goes beyond the small interval suggested by the neutron diffraction data (≈ 4 K). With this hypothesis, the (c_x,c_y,f_z) mode will start to nucleate at ≈ 70 K, which is the temperature at which the isothermal magnetization measurements indicate the appearance of a small ferromagnetic component. A similar behavior has been observed by some of us in Pr_2NiO_4,[13,14] where the (g_x,c_y,f_z) and (c_x,g_y,a_z) coexist in a temperature range of $\approx 100°$. A second possibility is related to the fact that our sample is nonstoichiometric. Then a mixture of irreducible representations is likely to occur. The magnetic structure between T_1 and T_{N2} will then be described by the $(g_x,g_y,f_z)=(g_x,g_y,0)+(0,0,f_z)$ mode, which is a basis function of a reducible representation of the direct sum $\Gamma_3(g_x,g_y,0)\oplus\Gamma_1(0,0,f_z) = \Gamma_3\oplus\Gamma_1(g_x,g_y,f_z)$. Finally, the third possibility is the existence of a change in the crystallographic space group below T_1. As was previously pointed out, no appreciable change in the crystallographic symmetry could be detected in the previous medium-resolution neutron-powder-diffraction experiments. Further high-resolution measurements would be needed in order to clarify this question.

In a wide temperature range, the isothermal magnetization curves $M(H_a)$ may be represented by the equation

$$M(H_a,T)=M_0(T)+\chi_{\rm dif}(T)H_a \ , \tag{3}$$

where $\chi_{\rm dif}(T)$ is the high-field differential susceptibility, H_a is the applied magnetic field, and $M_0(T)$ is the extrapolated spontaneous magnetization. The temperature dependence of $M_0(T)$ and the reciprocal of $\chi_{\rm dif}(T)$ are shown in Figs. 11 and 12. We see that $M_0(T)$ starts to depart from zero at about $T \approx 70$ K and it increases smoothly from 70 to 20 K. At this temperature, a sudden, strong increase is observed, which is followed by a small anomaly at $T_{N2} \approx 13.5$ K. The $T_3 \approx 12$ K feature is also clearly observed.

The behavior of $M_0(T)$ between 70 and 20 K describes the evolution of the weak ferromagnetic component of the Ni^{2+} magnetic moments along the c axis. This f_z component develops an out-of-plane component of the internal field that polarizes the Nd^{3+} magnetic moments (through the Nd-Ni interactions), which also contribute to the observed increase of the spontaneous magnetization. The sudden increase at 20 K indicates a strong enhancement of the $\mu_z^{\rm Nd}$ component, which, as will be shown later, is due to the strong uniaxial magnetocrystalline anisotropy associated with the Nd^{3+} ions.[6] At $T_{N2}=13.5$ K, the c-axis component of the internal mag-

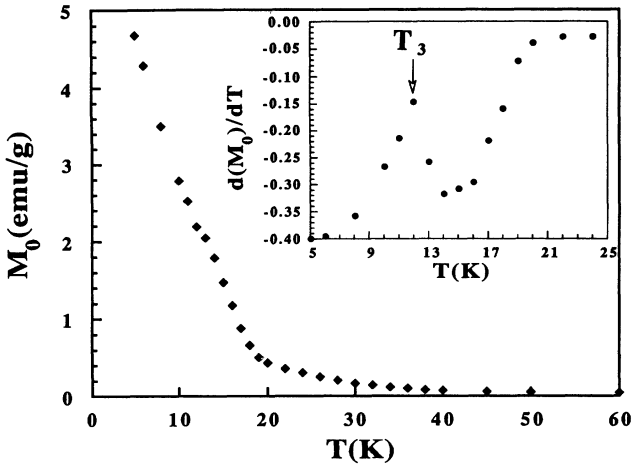

FIG. 11. Temperature dependence of the spontaneous magnetization M^0 extrapolated to $H=0$. Inset: $d(M^0)/dT$ showing the long-range antiferromagnetic ordering of the Nd moments.

netic field does not appear to be significantly modified by the long-range ordering of these ions [there is no abrupt change in $M_0(T)$ at T_{N2}]. This fact suggests that the Nd-Ni and Nd-Nd interactions do not compete with each other since both magnetic sublattices order in the same magnetic mode at low temperature [(c_x,c_y,f_z) for the Ni sublattice and (C_x,C_y,F_z) for the Nd sublattice] as in the case of the pure compound. This behavior is in sharp contrast to that observed in the T' cuprates, such as Gd_2CuO_4, where the internal magnetic field disappears when the antiferromagnetic long-range ordering of the Gd ions is approached.[15]

Finally, it should be pointed out that below 12 K, we observe a clear upturn in the isothermal magnetization at high fields, which we suggest has the same origin as that in the undoped $Nd_2NiO_{4.00}$ compound, i.e., a metamagnetic transition involving the antiparallel weak ferromagnetic components of Nd and Ni sublattices. Even though the determination of the critical field is not accessible with our experimental setup, all the characteristics indicate a similar value to that observed in $Nd_2NiO_{4.00}$.[6]

On the other hand, the inverse of the high-field differential susceptibility (see Fig. 12) shows again the T_3 and T_1 anomalies, related, respectively, to the long-range magnetic ordering of the Nd^{3+} ions at $T_{N2}=12$ K and the beginning of the in-plane reorientation of the Ni^{2+} magnetic moments at $T_{C1}\approx 130$ K. Above T_1 we observe a Curie-Weiss-like law with a magnetic moment matching that of free Nd^{3+} ions, namely, $\mu_{\text{eff}}\approx 3.26\mu_B$, since in this case the polarization effect of the external applied field is automatically subtracted.

Further support of these facts is given by looking at Fig. 13, where saturation magnetization $M_0(T)$ versus high-field differential susceptibility $\chi_{\text{dif}}(T)$ is depicted. This figure clearly shows that M_0 starts to develop below about 70 K, and confirms the existence of the 20-K anomaly in the extrapolated spontaneous magnetization. An additional anomaly is observed at ≈ 40 K.

V. DISCUSSION

A. Evaluation of the internal field acting on the Nd^{3+} ions and the canting of the Ni and Nd magnetic moments

As in the previous work on Nd_2NiO_4, we can evaluate the zero-field extrapolation of the internal field acting on the Nd^{3+} ions. To estimate its magnitude, we refer to Ref. 6 for writing Eq. (3) as

$$M^0(T)=M^0_{\text{Ni}}+\chi_{\text{dif}}(T)H_i^0 , \tag{4}$$

where H_i^0 is the internal field induced by the weak ferromagnetic component M^0_{Ni} of the Ni^{2+} magnetic moments. This relation is depicted in Fig. 13, where a linear dependence between $M^0(T)$ and $\chi_{\text{dif}}(T)$ in the temperature range from $T\approx 40$ K down to $T\approx 20$ K is evident. A determination of the slope and intercept gives

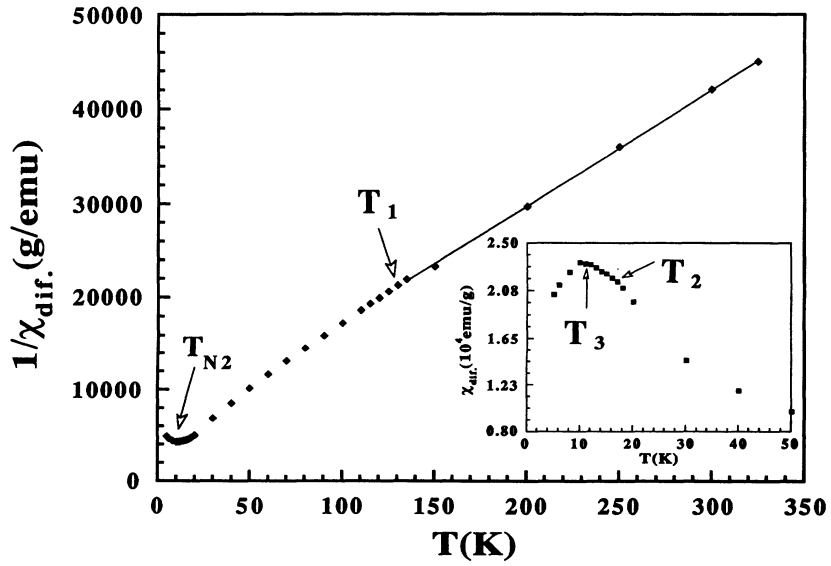

FIG. 12. Reciprocal of the high-field differential susceptibility as a function of temperature. Inset: detail of the low-temperature region showing a cusp of the dc susceptibility at T_{N2}.

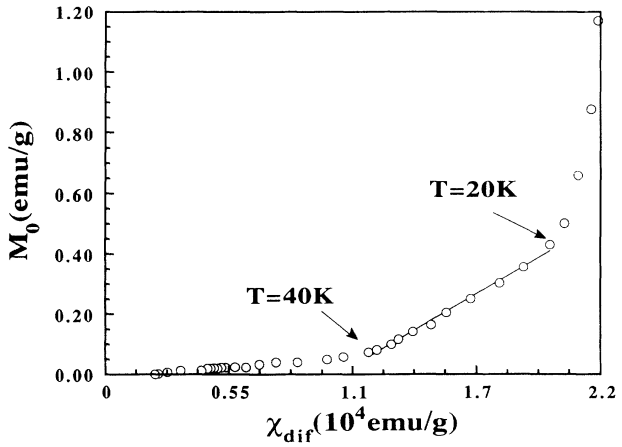

FIG. 13. Saturation magnetization $M^0(T)$ vs high-field differential susceptibility $\chi_{dif}(T)$ showing their linearity from 20 to 40 K.

$M^0_{Ni} \approx -0.03(4)\mu_B$/f.u. and $H_i^0 \approx 4.4(5)$ kOe. The negative sign of M^0_{Ni} indicates that the Nd-Ni interaction is antiferromagnetic. As we can see, the value of M^0_{Ni} is too small to be detected by neutron-powder diffraction. By using the total magnetic moment in the Ni sites obtained with this technique ($1.43\mu_B$ at $T=16.5$ K), we can estimate the angle between the Ni moments and the *ab* plane to be $\theta \approx 1.3(3)°$. Figure 13 depicts a very similar behavior to that observed in undoped $Nd_2NiO_{4.00}$,[6] but in this case, the values of the weak ferromagnetic component and the angle θ are strongly reduced ($\mu_z^{Ni} \approx -0.20\mu_B$ and $\theta \approx 13.1°$ in Nd_2NiO_4).

Within the framework developed in Ref. 6 and in the scope of the mean-field approximation, the obtained values of H_i^0 and M^0_{Ni} allow the determination of an isotropic Nd-Ni exchange of $J_{Nd\text{-}Ni} \approx -0.7(3)$ meV, which is very similar to the value obtained for $Nd_2NiO_{4.00}$.[6]

Finally, a strong increase of $M^0(T)$ is observed below 20 K, $M^0(T)$. As in the case of $Nd_2NiO_{4.00}$, it has been attributed to the increase of the strong uniaxial magnetocrystalline anisotropy associated to the Nd^{3+} ions.[6]

Concerning the Nd magnetic sublattice, we can estimate the value of the weak ferromagnetic component since when $H_a < H_{cr}$ the total saturation magnetization is given by

$$M_0 = 1.8M^0_{Nd} + M^0_{Ni} \ . \tag{5}$$

From our data, M_0 $(T \to 0) \approx 0.46\mu_B$/f.u. and $M^0_{Ni} \approx -0.03\mu_B$/f.u. independent of temperature. Since the total magnetic moment in the Nd sites obtained by neutron diffraction at $T \approx 1.5$ K is around $1.60\mu_B$ we determine that $M^0_{Nd} \approx 0.27\mu_B$ and the angle between the Nd moments and the *a-b* plane is $\theta' \approx 9.6(3)°$.

B. Magnetic interactions

In first approximation, the magnetic Hamiltonian describing the magnetic interactions in $Nd_{1.8}Sr_{0.2}NiO_{3.72}$ may be considered the same as that of the undoped $Nd_2NiO_{4.00}$ compound [see Eq. (10) of Ref. 6]. The magnetic structure of the compound may be parametrized through the canting angles of the Ni and Nd moments, θ and θ', respectively, with respect to the *a-b* plane. Thus, minimizing the system energy with respect to these parameters, the equilibrium state will be reached when

$$-4J_{Ni\text{-}Ni}S^{Ni}S^{Ni}\sin(2\theta) - 8J'_{Ni\text{-}Ni}S^{Ni}S^{Ni}\sin(2\theta) + 4D^{Ni\text{-}Ni}S^{Ni}S^{Ni}\cos(2\theta) - 10J_{Nd\text{-}Ni}S^{Ni}S^{Nd}\sin(\theta+\theta') = 0 \ , \tag{6}$$

$$4.5J_{Nd\text{-}Ni}S^{Ni}S^{Nd}\sin(\theta+\theta') - 3.6K^{Nd}\sin(\theta')\cos(\theta') = 0 \ . \tag{7}$$

Here $J_{Ni\text{-}Ni}$ represents the in-plane symmetric part of the antiferromagnetic Ni-Ni superexchange interaction and $\mathbf{D}_{Ni\text{-}Ni} = (0, D_{Ni\text{-}Ni}, 0)$ is the Dzyaloshinski-Moriya interaction.[16,17] $J'_{Ni\text{-}Ni}$ takes into account the magnetic interactions between two adjacent NiO_2 planes, while $J_{Nd\text{-}Ni}$ represents an effective isotropic Nd-Ni superexchange coupling constant. Finally, K^{Nd} represents the anisotropy energy per Nd spin and is related to the first anisotropy constant K_1^{Nd} through the volume V_{uc} and the number of Nd ions Z', of the unit cell,

$$K_1^{Nd} = K^{Nd}(Z'/V_{uc}) \ . \tag{8}$$

Regarding the values of the magnetic interactions ($J_{Ni\text{-}Ni}$, $J'_{Ni\text{-}Ni}$, and $J_{Nd\text{-}Ni}$), very few experimental determinations are reported in the literature. Aeppli and Buttrey[18] found that $J_{Ni\text{-}Ni} \approx -20$ meV in $La_2NiO_{4.00}$, a value that is expected to be slightly smaller [around 5% (Ref. 6)] in the case of $Nd_2NiO_{4.00}$ since the decrease of the superexchange Ni-O-Ni angle φ and the increase of the in-plane Ni-O distance d,[7,19] with respect to La_2NiO_4, tend to reduce the in-plane magnetic interaction. Using the same arguments, a decrease of $\approx 2\%$ (≈ 0.4 meV) with respect to the value in Nd_2NiO_4 is expected for $J_{Ni\text{-}Ni}$ in $Nd_{1.8}Sr_{0.2}NiO_{3.72}$. Because this variation is of the same order of magnitude as the expected error (≈ 0.3 meV), we have used the same value as that in the undoped $Nd_2NiO_{4.00}$ compound, that is, $J_{Ni\text{-}Ni} \approx -19$ meV (Ref. 6) for the rest of the discussion. Also, we have assumed that $J'_{Ni\text{-}Ni}$ is basically the same as that in Nd_2NiO_4.

Finally, from the measurements of $M^0(T)$ and H_i^0 we have obtained $J_{Nd\text{-}Ni} \approx -0.7$ meV, which is almost the same as that obtained in the undoped $Nd_2NiO_{4.00}$ compound. This concordance in the values of $J_{Nd\text{-}Ni}$ gives further support to our assumption that $J'_{Ni\text{-}Ni}$ is very similar in value in both the undoped and doped compounds.

The substitution of the five parameters $J_{Ni\text{-}Ni} \approx -19$ meV, $J'_{Ni\text{-}Ni} \approx -2.2$ meV, $J_{Nd\text{-}Ni} \approx -0.7$ meV, $\theta \approx 1.3°$, and $\theta' \approx 9.6°$ into Eqs. (6) and (7) allows the determination of $D_{Ni\text{-}Ni}$ and K^{Nd}, that is, $D_{Ni\text{-}Ni} \approx -1.4$ meV and $K^{Nd} \approx 2.3$ meV, which leads to a value of the first anisotropy constant $K_1^{Nd} \approx 0.8 \times 10^8$ erg/cm^3 for the Nd atoms.

When comparing these values with that obtained for

undoped $Nd_2NiO_{4.00}$, we see that both K_1^{Nd} and $D_{Ni\text{-}Ni}$ have been clearly reduced. The anisotropy constant has been reduced by a factor of 2. This reduction may be associated with the structural distortion introduced by the different size of Nd and Sr ions, which may affect the electronic distribution of the Nd ions and then to the single-ion-type magnetic anisotropy. On the other hand, if we compare the coercive fields of the undoped and doped compounds, we observe that the latter has been reduced by a factor of 50 (at $T=4.5$ K). This change cannot be explained by the reduction of the uniaxial magnetic anisotropy of the Nd ions alone, but mostly by the small values of the weak ferromagnetic components.

Finally, the antisymmetric interaction $D_{Ni\text{-}Ni}$ has been reduced by a factor of ≈ 10 with respect to the value calculated in the undoped compound.[6] This strong reduction arises from the strong sensitivity to the variations of the tiling angle of the octahedra, which has been reduced from $\simeq 9°$ in Nd_2NiO_4 to $\simeq 6°$ in $Nd_{1.8}Sr_{0.2}NiO_{3.72}$.

VI. CONCLUSIONS

The main conclusion of this work is that, in spite of (a) the considerable amount of partially ordered oxygen vacancies in $Nd_{1.8}Sr_{0.2}NiO_{3.72}$ (14% of the basal oxygens) and (b) the lower symmetry of this compound ($B112/n$) with respect to Nd_2NiO_4 ($Bmab$), the magnetic behavior of both nickelates shows very strong similarities, at least in the $RT > T > 13.5$ K temperature range. Below 13.5 K the situation is substantially different. Although some details of the low-temperature magnetic structure have still to be clarified, the observed magnetic arrangement is very different from that reported for Nd_2NiO_4 and $Nd_{1.95}Sr_{0.05}NiO_4$ in the same range of temperatures.

The structural and electronic changes produced by Sr doping and the oxygen vacancies seem then to affect predominantly the ground state of the rare earth and, more concretely, their single-ion anisotropy. The Ni-Ni coupling appears to be less sensible to this kind of effect, even the local environment of the Ni atoms is more affected by the O vacancies than that of Nd. In fact, only the Dzyaloshinsky-Moriya interaction, much more sensible to the structural modifications, has been found to be affected in a significative way.

ACKNOWLEDGMENTS

We would like to thank the Institut Laue-Langevin for the allocation of beam time, as well as our colleagues M. Vallet-Regí, J. M. González-Calbet, and J. Alonso for the synthesis of the sample used in this work. One of us (M.M.) thanks also the Spanish Ministry of Education and Science for supporting her visit to France.

*Present address: Laboratorium für Neutronenstreuung, ETH and PSI, 5332 Villigen PSI, Switzerland.

†Present address: Laboratoire Léon Brillouin (CEA/CNRS) 91191 Gif sur Yvette Cedex, France.

[1]M. Medarde, J. Rodríguez-Carvajal, M. Vallet-Regí, J. González-Calbet, and J. Alonso, this issue, Phys. Rev. B **49**, 8591 (1994).

[2]M. Crespin, J. M. Bassat, P. Odier, M. Mouron, and J. Choisnet, J. Solid State Chem. **84**, 165 (1900).

[3]M. Crespin, J. Solid State Chem. **100**, 281 (1992).

[4]M. Medarde, Ph.D. thesis, Universidad de Barcelona, 1992.

[5]M. Medarde, J. Rodríguez-Carvajal, X. Obradors, M. Vallet-Regí, J. M. González-Calbet, and J. Alonso, Physica B **180&181**, 402 (1992).

[6]X. Batlle, X. Obradors, and B. Martínez, Phys. Rev. B **45**, 2830 (1992).

[7]J. Rodríguez-Carvajal, M. T. Fernández-Díaz, J. L. Martínez, F. Fernández, and R. Sáez-Puche, Europhys. Lett. **11**, 261 (1990).

[8]K. Yamada, M. Matsuda, Y. Endoh, B. Keimer, R. J. Birgeneau, S. Onodera, J. Mizusaki, T. Matsuura, and G. Shirane, Phys. Rev. B **39**, 2336 (1989).

[9]S. Kirpatrick, Rev. Mod. Phys. **45**, 574 (1973).

[10]J. Rodríguez-Carvajal, Physica B **192**, 55 (1993).

[11]C. L. Seaman, N. Y. Ayoub, T. Bjornholm, E. A. Early, S. Ghamaty, B. W. Lee, J. T. Market, J. J. Neumeier, P. K. Tsai, and M. B. Maple, Physica C **159**, 391 (1989).

[12]X. Batlle, X. Obradors, M. J. Sayagués, M. Vallet, and J. Gonzálex-Calbet, J. Phys. Condens. Matter **4**, 487 (1992).

[13]M. T. Fernández-Díaz, J. Rodríguez-Carvajal, J. L. Martínez, G. Fillion, F. Fernández, and R. Sáez-Puche, Z. Phys. B **82**, 275 (1991).

[14]M. T. Fernández-Díaz, J. L. Martínez, J. Rodríguez-Carvajal, J. Beille, B. Martínez, X. Obradors, and P. Odier, Phys. Rev. B **47**, 5834 (1993).

[15]J. D. Thompson, S. W. Cheong, S. E. Brown, S. Fisk, S. B. Oseroff, M. Tovar, D. C. Vier, and S. Shultz, Phys. Rev. B **39**, 6660 (1989).

[16]I. Dzyaloshinski, J. Phys. Chem. Solids **4**, 241 (1958).

[17]T. Moriya, Phys. Rev. **120**, 91 (1960).

[18]G. Aeppli and D. J. Buttrey, Phys. Rev. Lett. **61**, 203 (1988).

[19]J. Rodríguez-Carvajal, M. T. Fernández-Díaz, and J. L. Martínez, J. Phys. Condens. Matter **3**, 3215 (1991).

[20]E. F. Bertaut, Acta Crystallogr. **A24**, 217 (1968); see also from the same author: *Spin Configurations of Ionic Structures: Theory and Practice*, in *Magnetism*, edited by G. T. Rado and H. Suhl (Academic, New York, 1963), Vol. 3, p. 150.